



Ipomoea aquatica root as a new potential adsorbent to remove methyl violet 2B dye in simulated dye contaminated wastewater

Yie Chen Lu^a, N. Priyantha^{b,c}, Linda B.L. Lim^{a,*}, Abdul Hanif Mahadi^d,
Nuraina Afiqah Mohammad Zain^d

^aChemical Sciences Programme, Faculty of Science, Centre for Advanced Material and Energy Sciences, Universiti Brunei Darussalam, Negara Brunei Darussalam, Tel. +00-673-8748010; emails: linda.lim@ubd.edu.bn (L.B.L. Lim), yiechen_93@hotmail.com (Y.C. Lu)

^bDepartment of Chemistry, Faculty of Science, University of Peradeniya, Peradeniya, Sri Lanka, email: namal.priyantha@yahoo.com (N. Priyantha)

^cPostgraduate Institute of Science, University of Peradeniya, Peradeniya, Sri Lanka

^dCentre for Advanced Material and Energy Sciences, Universiti Brunei Darussalam, Negara Brunei Darussalam, emails: hanif.mahadi@ubd.edu.bn (A.H. Mahadi), 18m2781@ubd.edu.bn (N.A.M. Zain)

Received 5 November 2019; Accepted 3 April 2020

ABSTRACT

Ipomoea aquatica, a popular vegetable that has also been used in the decontamination of wastewater, is investigated in this study. By turning its root, which is normally thrown away as waste, into a useful adsorbent makes it possible for the removal of toxic methyl violet 2B (MV) dye. When analyzed with different models and error functions, adsorption isotherm data best fitted to the Sips model. The adsorption process was found to follow pseudo-second-order kinetics with an apparent rate constant of 22.10 g mmol⁻¹ min⁻¹. The thermodynamic study pointed to a spontaneous, endothermic adsorption process (ΔH° 9.66 kJ mol⁻¹). High maximum adsorption capacity of 354.6 mg g⁻¹, short time to reach equilibrium, as well as its relatively good resilience when placed in an environment with different pH and ionic strengths all lend support to *I. aquatica* roots being a strong, low-cost adsorbent in wastewater treatment. Another attractive feature is its ability to be regenerated and reused yet maintaining strong adsorption characteristics after many cycles, with and without any treatment of the spent adsorbent.

Keywords: *Ipomoea aquatica* (water spinach) root; Methyl violet 2B dye; Adsorption isotherm; Kinetics; Thermodynamics; Regeneration

1. Introduction

Ever-increasing demands for food and material goods by the rapidly growing world population have resulted in both agricultural and industrial wastes being disposed of, often recklessly without proper pre-treatment, thereby causing a detrimental impact on the environment we live in. Contaminated water, if untreated, affects both aquatic and human alike. Depending on the level of toxic pollutants, it can even result in fatality. Hence, there is an urgent need

to clean up wastewater pollution in order to ensure the availability and consumption of safe drinking water.

The last decade has seen the emergence of various methods to tackle the problems of wastewater pollution. Amongst these methods, adsorption has gained popularity as it provides a quick, inexpensive, simple, and yet effective method to remove pollutants, such as dyes and heavy metals. Various adsorbents have been tested out, ranging from waste derived from agriculture [1–3], industries [4,5], and food [6] to biomasses, such as leaves [7] and peat [8–10].

* Corresponding author.

Synthetic and modified adsorbents have also received much attention in recent years, leading to excellent adsorption ability [11,12]. However, it must be stressed that not all synthesized or modified adsorbents showed enhanced adsorption capacity compared to natural adsorbents [13–15]. In fact, many natural adsorbents have far superior adsorption ability. Hence in this respect, the search for natural adsorbents is still in demand as these adsorbents are more cost-effective and easily accessible without having to be generated from complicated laboratory procedures.

Ipomoea aquatica, known as Kangkong by the locals in Brunei Darussalam, is a tropical semi-aquatic plant very commonly found growing along the roadside and in ditches, but it is also cultivated and sold in local open markets. It is a very popular and cheap vegetable which is available throughout the year. Reports have shown that *I. aquatica* has the ability to effectively phytoremediate various heavy metals [16–20], organic contaminants [21], and dye [22]. Further, studies have also shown that *I. aquatica* was able to improve the aquaculture wastewater quality [23] and eutrophic lake [24]. However, its use as an adsorbent in adsorption studies has not been widely reported. A recent study demonstrated the successful use of the stalks of *I. aquatica* to adsorb dye. To the best of our knowledge, its roots have never been tested and this is the first study on its use as an adsorbent.

The model dye chosen in this investigation is the methyl violet 2B dye (MV). Being corrosive, if ingested or contacted MV may cause severe damage to eyes, inhalation difficulty, and skin irritation [25]. It is also known to be hazardous to aquatic life. Hence, there is a need for its removal from contaminated wastewater. Even though *I. aquatica* has been used in phytoremediation to remove dyes, the dye tested was diazo dye Brown 5R [22]. Its use as an adsorbent to remove MV has never been reported. This work, therefore, will be the first such report on the use of *I. aquatica* root as a new, potential, and low-cost adsorbent for the adsorption of dye. Another attractive feature of this adsorbent is that it requires very mild preparation conditions, yet exhibits strong adsorption capability of the MV dye. This research also aimed to provide an insight into the adsorption characteristics of this adsorbent such as the effects of ionic strength, pH, temperature, dye concentrations, and adsorption kinetics.

2. Materials and methods

2.1. Adsorbent preparation and chemical reagents

I. aquatica (Kangkong) was randomly selected from vegetable vendor stalls in the local open market. The Kangkong root (KR) was separated from the rest of the vegetable and washed under tap water several times followed by rinsing with distilled water to remove any dirt. Thereafter, the KR was placed in an oven at 65°C and dried until a constant mass was obtained. The dried KR was blended using a household blender and sieved using laboratory stainless steel brass sieve to obtain the desired particle size of <355 µm. The powdered KR was stored under air-tight conditions until ready to be used.

The adsorbate chosen in this study was methyl violet 2B (MV) dye, also known as Basic violet 1, with molecular

formula $C_{24}H_{28}N_3Cl$ and M_r 393.96 mol g^{-1} , and was procured from Sigma-Aldrich (Germany) and used without further purification.

2.2. Sorption experiments

All experiments carried out in this study were done using 0.020 g of adsorbent in 10.0 mL of MV solution, keeping the mass:volume ratio as 1:500, unless otherwise stated. Agitation of the adsorbent–adsorbate mixture was set at 250 rpm and carried out at room temperature, except for thermodynamics studies where adsorption were investigated at temperatures of 298, 313, 323, 333, and 343 K. Except for adsorption isotherms which were carried out using MV dye concentrations ranging from 0 to 1,000 mg L^{-1} , all other experiments were carried out using 100 mg L^{-1} MV.

Effect of contact time was carried out at every 30 min interval for a total of 4 h in order to determine the time required for KR–MV system to reach equilibrium. Investigation of ionic strength was done using NaCl ranging from 0 to 1.0 M, while the effect of pH was performed between pH 2 and 12. All experiments were done by shaking the KR–MV mixtures for optimal shaking time, obtained from the effect of contact time, except for kinetics studies whereby every 1 min interval was used for the first 10 min and thereafter at every 3 min interval from 12 min onwards.

Determination of the best-fit isotherm and kinetics models for the adsorption of MV onto KR was analyzed using five error functions, that is, the average relative error (ARE), the sum square error (SSE), the sum of absolute error (EABS), the Marquart's percent standard deviation (MPSD), and chi-square test (χ^2), as shown below by Eqs. (1)–(5), respectively.

$$\frac{100}{n} \sum_{i=1}^n \left| \frac{q_{e,meas} - q_{e,calc}}{q_{e,meas}} \right|_i \quad (1)$$

$$\sum_{i=1}^n (q_{e,calc} - q_{e,meas})_i^2 \quad (2)$$

$$\sum_{i=1}^n |q_{e,meas} - q_{e,calc}| \quad (3)$$

$$100 \sqrt{\frac{1}{n-p} \sum_{i=1}^n \left(\frac{q_{e,meas} - q_{e,calc}}{q_{e,meas}} \right)_i^2} \quad (4)$$

$$\sum_{i=1}^b \frac{(q_{e,meas} - q_{e,calc})^2}{q_{e,meas}} \quad (5)$$

2.3. Instrumentation

The absorbance of MV was measured using Thermo Scientific Genesys 20 UV-visible spectrophotometer, USA, set at the wavelength 584 nm. The surface area was obtained using the Brunauer–Emmett–Teller (BET) Micromeritics

ASAP™ 2020, USA. The surface morphology of KR, before and after adsorption of MV, was carried out using the Quanta 400, FEI, scanning electron microscopy (SEM, Czech Republic). Fourier transform infrared (FTIR) spectroscopy (Model: Agilent Cary 630 FTIR spectrometer, USA) was used to determine the functional groups present in the adsorbent.

3. Results and discussion

3.1. Characterization of KR

Characterization of KR using BET revealed its surface area to be $0.4250 \text{ m}^2 \text{ g}^{-1}$, which was significantly reduced to $0.0551 \text{ m}^2 \text{ g}^{-1}$ upon adsorption of MV. The surface morphology of KR, before and after adsorption of MV, is shown by the SEM images in Fig. 1. Before adsorption of MV, KR showed a combination of rough, uneven surface with some crystalline-like structures, whereas upon adsorption of the dye, noticeable changes on the surface of KR could be observed. The MV-loaded KR appeared much smoother and flat, and the surface appeared to be more even as compared to the situation prior to adsorption of the dye, which supports the observations made on strong adsorption of MV on KR (Fig. 1).

Insight into the possible functional groups present in KR that may be involved in the adsorption process was determined from the FTIR spectra. From Fig. 2, a very prominent change occurred in the broad OH peak at $3,420 \text{ cm}^{-1}$. A significant shift of C=O from $1,734$ to $1,756 \text{ cm}^{-1}$ was also observed. The C–H peak at $2,906 \text{ cm}^{-1}$ was slightly shifted to $2,901 \text{ cm}^{-1}$, while the peak at $1,647 \text{ cm}^{-1}$ was shifted to $1,653 \text{ cm}^{-1}$ which could be attributed to C=C and C=N. Peak at $1,165 \text{ cm}^{-1}$ is indicative of C–N stretching of the MV dye.

3.2. Effect of contact time

Investigation on the relationship of dye removal-shaking time performed over a 4 h period clearly indicates that rapid adsorption of >70% MV by KR occurs within the first half an hour, owing to the availability of empty vacant sites present on the surface of KR which allows

adsorption of dye to take place readily. The time taken for adsorption of MV by KR to reach equilibrium is fast, as observed in Fig. 3, unlike sunflower seed hull [25] and $\text{SnO}_2/\text{activated carbon fiber (ACF)}$ hybrid catalyst [26] which reportedly required 105 minutes and >10 h, respectively. Fast equilibrium attained by KR indicates that the resistance to mass transfer of MV between the solid and aqueous phases could be easily overcome. The ability of KR–MV system to reach equilibrium quickly is an advantage economically since the shorter the time, the more cost-saving it will be when applied in the wastewater treatment plant.

3.3. Kinetics studies of adsorption of MV on KR

Insight into the mechanism of adsorption kinetics was elucidated with the application of three commonly used kinetics models, namely the Lagergren pseudo-first-order [27], pseudo-second-order [28], and the Elovich [29] models. Linearized forms of the above models are shown in Eqs. (6)–(8), respectively. The Lagergren pseudo-first-order and the pseudo-second-order kinetics are the most widely used models in adsorption studies. The Elovich model, first proposed by Roginsky and Zeldovich [29], is commonly applied to chemisorption processes where the adsorbent surface is heterogeneous.

$$\log(q_e - q_t) = \log(q_e) - \frac{k_1}{2.303} t \quad (6)$$

$$\frac{t}{q_t} = \frac{1}{k_2 q_e^2} + \frac{1}{q_e t} \quad (7)$$

$$q_t = \frac{1}{\beta} \ln(\alpha\beta) + \frac{1}{\beta} \ln t \quad (8)$$

In Eqs. (6)–(8), the rate constants for pseudo-first- and second-order kinetics are presented by k_1 and k_2 , respectively;

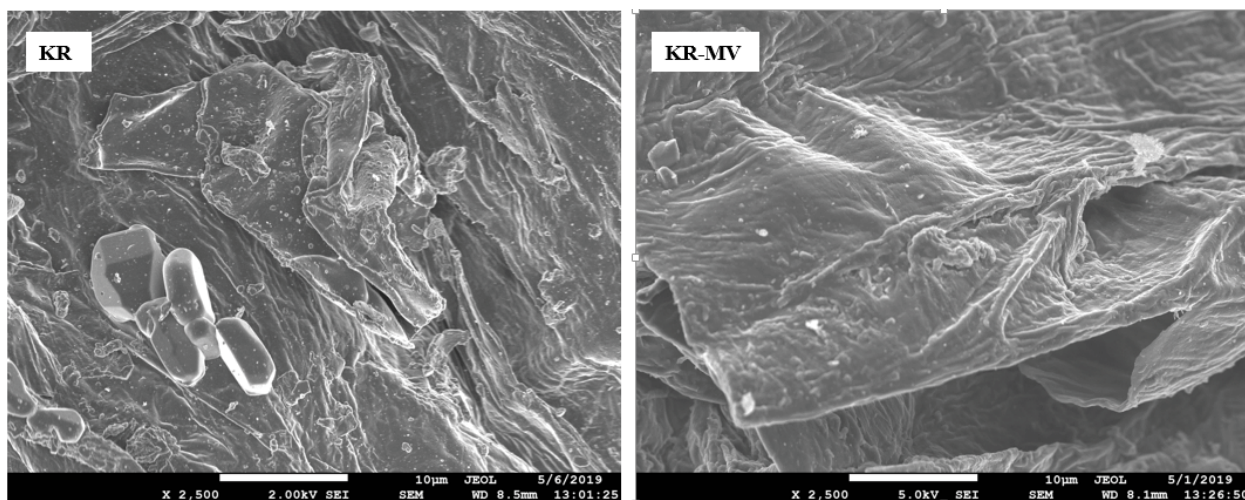


Fig. 1. SEM images showing surface morphology of KR before and after loaded with MV dye under 2,500x magnification.

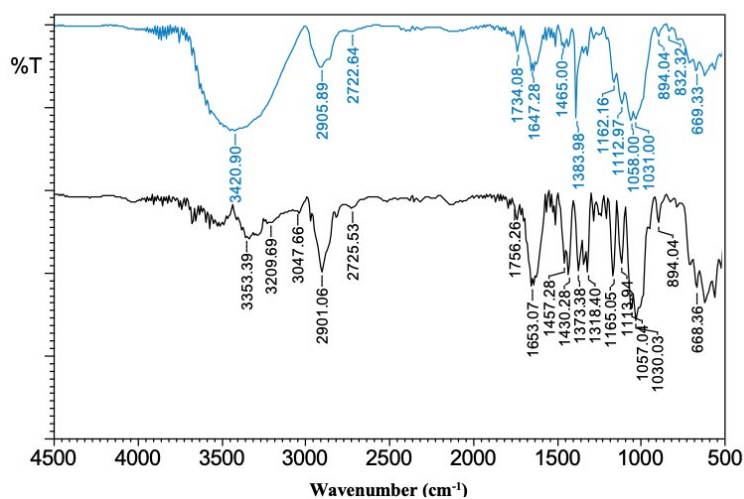


Fig. 2. IR spectra of KR (blue) and KR–MV (black).

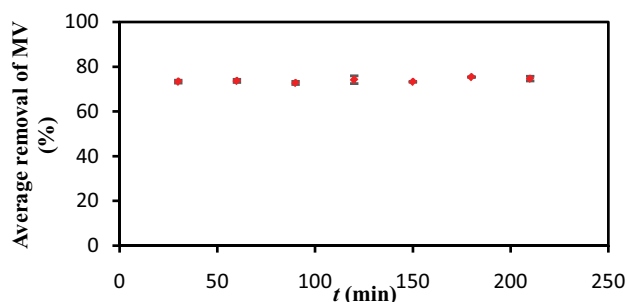


Fig. 3. Effect of contact time on adsorption of MV onto KR (mass of adsorbent = 0.020 g, concentration of MV = 100 mg L⁻¹, and volume of MV dye solution = 10.0 mL).

t is the time and q_t and q_e are the amounts of MV adsorbed at time t and at equilibrium, respectively.

Pseudo-order conditions in kinetics require changing the concentration of one reactant while that of other reactants is essentially made unchanged. This condition for adsorption–adsorbate reactions can be achieved by monitoring the adsorption rate during the initial period of interaction. Therefore, the extent of adsorption measurements of MV on the adsorbent within the first 20 min was used for kinetics analysis. Of the three linear plots as shown in Figs. 4a–c, the pseudo-second-order kinetics gave the highest R^2 close to unity, when compared to the Lagergren pseudo-first-order ($R^2 < 0.10$) and Elovich ($R^2 < 0.61$) models. This is further supported by the comparison of experiment kinetics data with the simulated models, as shown in Fig. 4d, where a large deviation of the Lagergren pseudo-first-order kinetics was observed. Although the Elovich model appeared to be a close fit to the experiment data, its low R^2 suggests otherwise. Another factor that supports the pseudo-second-order kinetics is its compatible value of calculated adsorption capacity (q_{cal}) with the experiment (q_{expt}), as indicated in Table 1. As the pseudo-order condition is applied on the adsorbate (MV dye), fulfilling the requirements of the pseudo-second-order kinetics can be attributed

to having two distinct types of reactive moieties in the adsorbent to interact with MV [30]. The extent of adsorption, that is, the removal, cannot be addressed from kinetics measurements, and investigation of adsorption equilibrium aspects would provide such information. Nevertheless, results of kinetics experiments performed under static conditions would provide preliminary information which would be much useful in extending the adsorbate–adsorbent system under investigation toward large scale treatment processes to remove MV from contaminated water. However, more experimental and process parameters would have to be optimized in such applications.

Natural adsorbents, such as KR used in this investigation, have heterogeneous surfaces and can be treated as a three-dimensional structure with an extensive network of pores having a wide range of depths and diameters, indicating the possibility of many modes of mass transfer. As some pores could be deep, diffusion aspects should also be considered as an important factor to account for adsorption kinetics [31]. Consequently, the validity of diffusion models should be investigated, and in this respect, the Weber–Morris intra-particle diffusion model, represented as Eq. (9) would provide valuable information:

$$q_t = k_i t^{1/2} + C \quad (9)$$

where k_i is the intraparticle diffusion rate constant (mmol g⁻¹ min^{-0.5}) and C is a measure of the thickness of the boundary layer.

The plot of the amount of MV adsorbed q_t vs. $t^{1/2}$ is indicative of three linear portions, as observed in many heterogeneous adsorbent surfaces (Fig. 5), which could be attributed to fast external adsorption onto the adsorbent surface, followed by gradual adsorption step controlled by intra-particle diffusion, and thereafter, the final equilibrium step where the adsorbent moves slowly from larger pores to micropores resulting in a slow adsorption rate [32]. The constant C , which is a measure of the thickness of the boundary layer, determined by extrapolating Fig. 5b is 0.084, includes MV molecules before being adsorbed on to KR.

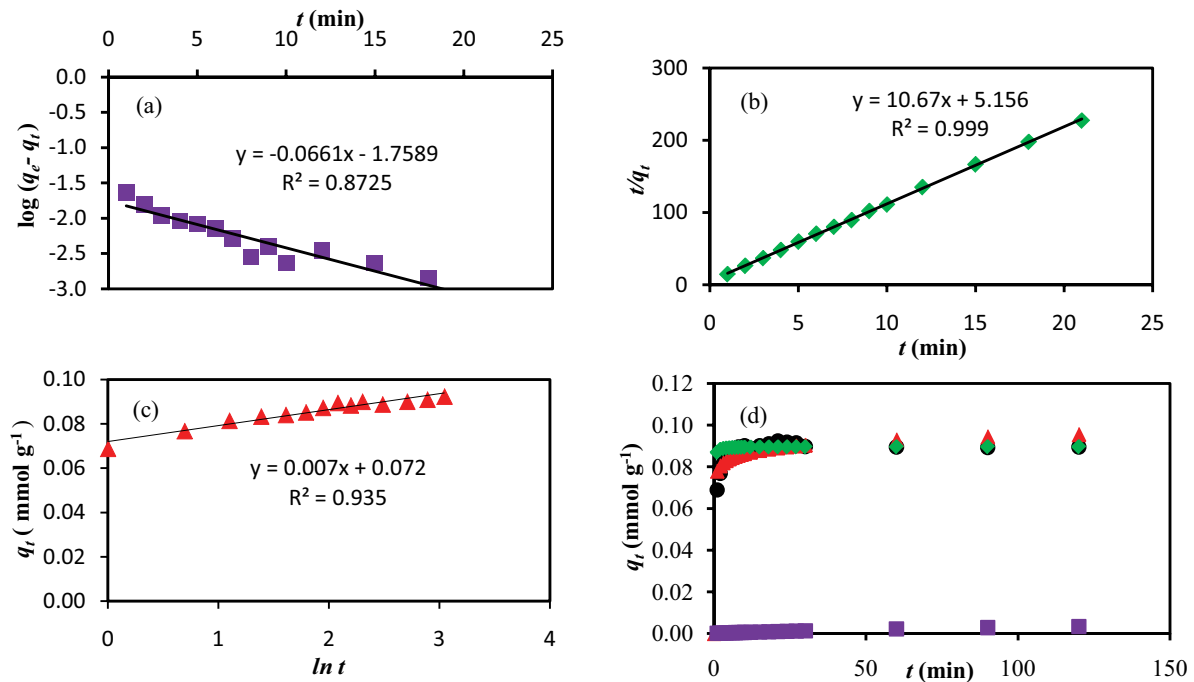


Fig. 4. Linear plots of (a) Lagergren pseudo-first-order, (b) pseudo-second-order, (c) Elovich kinetics models for the adsorption of MV by KR, and (d) comparison of experiment kinetics data (•) with the non-linear plots of Lagergren pseudo-first-order (■), pseudo-second-order (◆), and Elovich (▲) kinetics models (mass of adsorbent = 0.020 g, concentration of MV = 100 mg L⁻¹, and volume of MV dye solution = 10.0 mL).

Table 1

Parameters and error values of Lagergren pseudo-first-order kinetics, pseudo-second-order kinetics, and Elovich models on adsorption of MV with KR

Kinetics model	Parameter	ARE	SSE	EABS	MPSD	χ^2
Pseudo-first-order		87.39	0.08	1.04	94.51	0.91
	q_{expt} (mmol g ⁻¹)	0.102				
	q_{calc} (mmol g ⁻¹)	0.017				
	k_1 (min ⁻¹)	0.152				
	R^2	0.8725				
Pseudo-second-order		1.49	0.00	0.02	2.66	0.00
	q_{expt} (mmol g ⁻¹)	0.102				
	q_{calc} (mmol g ⁻¹)	0.094				
	k_2 (g mmol ⁻¹ min ⁻¹)	22.102				
	R^2	0.9997				
Elovich		3.23	0.00	0.04	4.81	0.00
	α (mmol g ⁻¹ min ⁻¹)	161.74				
	β (g mmol ⁻¹)	139.03				
	R^2	0.9359				

3.4. Adsorption isotherm and thermodynamics studies

Results of batch adsorption isotherm experiments carried out using 0–1,000 mg L⁻¹ MV dye at room temperature analyzed using three 2-parameter isotherm models (Langmuir, Freundlich, and Temkin) and two 3-parameter models (Redlich–Peterson and Sips) are shown in Table 2. Determination of the best isotherm model was done using

linear plots of these models, where higher R^2 generally indicates the better-fit model. Confirmation is then made through the use of five error functions, where the model with the lowest error values is indicative of the best-fit model, and from comparison of the experiment data with simulation plots of these models (Fig. 6, Table 3). The results point toward the Sips isotherm being the best model to describe the adsorption process under investigation. This model is

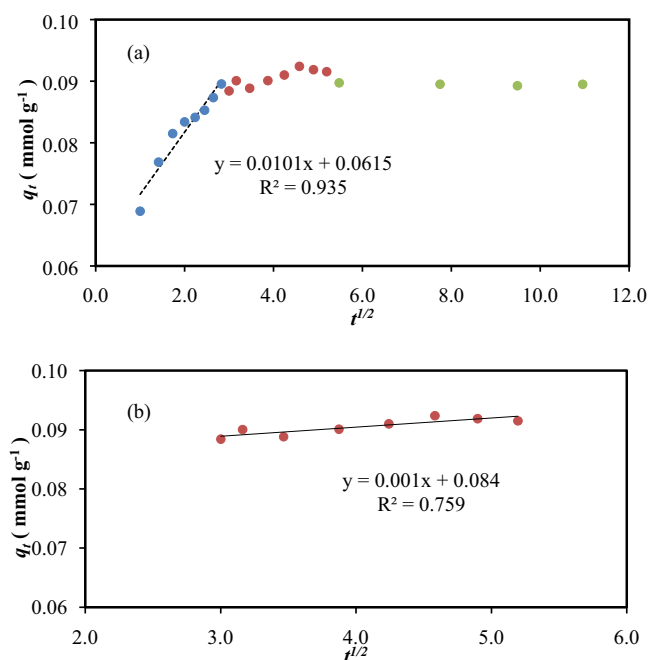


Fig. 5. Linear plot of Webber–Morris intra-particle diffusion model (a) a wide range in contact time and (b) intra-particle diffusion controlled region (mass of adsorbent = 0.020 g and volume of MV dye solution = 10.0 mL).

also known as the Langmuir–Freundlich model as it has the characteristics of both these models. The Sips model tends toward the Langmuir at high adsorbate concentrations and toward the Freundlich when the adsorbate concentrations are low. Based on the Sips isotherm, the maximum adsorption capacity (q_{max}) of KR in this study was found to be 354.6 mg g⁻¹. It should be stressed that an important application of isotherm studies, which are performed upon the system has reached equilibrium, is to estimate the extent of adsorption (i.e., removal) of the adsorbate, which would be extremely valuable in designing large-scale treatment plants.

In comparison with some other reported adsorbents, as indicated in Table 3, it is clear that the ability of KR to adsorb MV is superior. Further, its adsorption capability was compatible and, in many cases, better than activated carbon, synthesized materials, and chemically modified adsorbents. It must also be emphasized that KR used in this study was only subjected to drying at low heat (~60°C). Both the adsorbent and the adsorbate being organic in nature having polar functional groups would lead to strong adsorbate–adsorbent attractions leading to high extent of removal. It should also be stressed that there are still many more possibilities for further enhancement of its adsorption capacity through physical and/or chemical means [33].

In designing an effective adsorption system for real life application of wastewater treatment, adsorption thermodynamics is also vital as it provides valuable parameters for the

Table 2
Different isotherm models used, their linear equations, isotherm constants, and error values

Isotherm model and parameters	Values	
Langmuir $\frac{C_e}{q_e} = \frac{1}{K_L q_{max}} + \frac{C_e}{q_{max}}$		C_e and q_e are the concentration and adsorption capacity at equilibrium, respectively; K_L is the Langmuir constant and q_{max} is the maximum adsorption capacity
Plot $\frac{C_e}{q_e}$ vs. C_e		
q_{max} (mmol g ⁻¹)	1.032	
K_L (L mmol ⁻¹)	0.004	
R^2	0.9174	
ARE	12.35	
SSE	0.04	
EABS	0.51	
MPSD	22.58	
χ^2	0.29	
Freundlich $\log q_e = \frac{1}{n} \log C_e + \log K_F$		K_F is the Freundlich constant indicative of adsorption capacity; n is related to the adsorption intensity
Plot $\log q_e$ vs. $\log C_e$		
K_F (mmol g ⁻¹ (L mmol ⁻¹) ^{1/n})	0.008	
N	1.324	
R^2	0.9665	
ARE	14.64	
SSE	0.08	
EABS	0.67	
MPSD	27.14	
χ^2	0.41	

Isotherm model and parameters	Values	
Temkin $q_e = \left(\frac{RT}{b_T}\right) \ln K_T + \left(\frac{RT}{b_T}\right) \ln C_e$		K_T is the Temkin constant; b_T is related to the heat of adsorption; R is the gas constant while T is the absolute temperature at 298 K
Plot q_e vs. $\ln C_e$		
K_T (L mmol ⁻¹)	0.086	
b_T (kJ mol ⁻¹)	13.328	
R^2	0.9589	
ARE	42.39	
SSE	0.04	
EABS	0.64	
MPSD	92.60	
χ^2	0.46	
Redlich-Peterson $\ln\left(\frac{K_R C_e}{q_e} - 1\right) = n \ln C_e + \ln a_R$		K_R and a_R are the R-P constants and n is the empirical parameter related to the adsorption intensity
Plot $\ln\left(\frac{K_R C_e}{q_e} - 1\right)$ vs. $\ln C_e$		
K_R (L g ⁻¹)	0.020	
α	0.282	
a_R (L mmol ⁻¹)	1.771	
R^2	0.7605	
ARE	14.15	
SSE	0.07	
EABS	0.66	
MPSD	26.93	
χ^2	0.40	
Sips $\ln\left(\frac{q_e}{q_{\max} - q_e}\right) = \frac{1}{n} \ln C_e + \ln K_s$		K_s is the Sips constant; n is the Sips exponent
Plot $\ln\left(\frac{q_e}{q_{\max} - q_e}\right)$ vs. $\ln C_e$		
q_{\max} (mmol g ⁻¹)	0.900	
K_s (L mmol ⁻¹)	0.003	
n	0.874	
R^2	0.9789	
ARE	8.65	
SSE	0.02	
EABS	0.34	
MPSD	18.35	
χ^2	0.22	

designing process. The effect of temperature on the removal of MV by KR was investigated with temperature ranging from 298 to 343 K, and the thermodynamics parameters were obtained using Eqs. (10)–(13). The van't Hoff plot of $\ln K$ vs. T^{-1} points toward an endothermic adsorption process, as indicated by the positive enthalpy (ΔH°) (Fig. 7). Dissociative mechanism could also be involved as indicated by its positive entropy (ΔS°) in Table 4, showing more disorder, and therefore, adsorption is deemed favorable at higher temperatures. Increasing negativity in the Gibbs free energy (ΔG°) with increasing temperature confirms the spontaneity of the adsorption process.

$$\Delta G^\circ = \Delta H^\circ - T\Delta S^\circ \quad (10)$$

$$\Delta G^\circ = -RT \ln K \quad (11)$$

$$K = \frac{C_s}{C_e} \quad (12)$$

$$\ln K = \frac{\Delta S^\circ}{R} - \frac{\Delta H^\circ}{RT} \quad (13)$$

Table 3

List of the adsorption capacity (q_{\max}) values comparison for the removal of MV dye by KR and several reported adsorbents

Adsorbent	q_{\max} (mg g ⁻¹)	Reference
<i>Ipomoea aquatica</i> roots (KR)	354.6	This study
<i>Lemna minor</i> (Duckweed)	419.8	[34]
<i>Pistia stratiotes</i> L. (Water lettuce)	267.6	[35]
Almond shell	29.4	[36]
Poly-melamine-formaldehyde	113.9	[37]
<i>Casuarina equisetifolia</i> needle	165.0	[38]
Cempedak durian peel	238.5	[39]
<i>Artocarpus odoratissimus</i> skin	137.3	[40]
Pu-erh Tea powder (40 mesh)	277.8	[41]
<i>Nepenthes rafflesiana</i> pitcher	288.7	[42]
Pomelo skin	468.3	[43]
Pomelo leaves	248.2	[44]
Acid modified <i>Saccharum bengalense</i>	7.3	[45]
<i>Artocarpus odoratissimus</i> leaves	139.7	[33]
<i>Artocarpus odoratissimus</i> leaf-based cellulose	187.0	[46]
Halloysite-magnetite-based composite (HNT-Fe ₃ O ₄)	20.0	[47]
Granulated activated carbon	95.0	[48]
Granulated mesoporous carbon	202.8	[49]
Uncalcined Cu/Al LDH material	361.0	[50]
Soya bean waste	180.7	[51]

Table 4

Various thermodynamic parameters

Parameter	Temperature (K)				
	298	313	323	333	343
ΔG° (kJ mol ⁻¹)	-18.47				
ΔH° (kJ mol ⁻¹)	9.66	-19.88	-20.64	-21.61	-22.82
ΔS° (J mol ⁻¹ K ⁻¹)	94.25				

3.5. Effects of ionic strength and pH on adsorption of MV onto KR

Presence of ions in solution has been known to drastically reduce adsorption on the adsorbent surface. For instance, *Artocarpus odoratissimus* stem axis and jackfruit seed reported a reduction of about 17% and 23% removal toward MV, respectively, in 0.8 M NaCl [52,53]. Over the range of salt concentration (0–1.0 M) being investigated in this study, KR exhibited its ability to maintain a relatively good overall removal of MV, with a slight reduction of only 8% at 1 M NaCl as shown in Fig. 8 (top). This slight reduction in the removal of MV can be explained by the interference of Na⁺ ions, whereby competition of the cationic ions causing reduction in the electrostatic potential on the surface of KR. The presence of Na⁺ ions would also result in electrostatic repulsion of the cationic dye, MV, from the surface of KR, through compression of the electric double layer. Since wastewater usually contains many types of salts, an adsorbent that is able to withstand the effects of ionic strength while maintaining good adsorption ability is of vital importance in wastewater treatment.

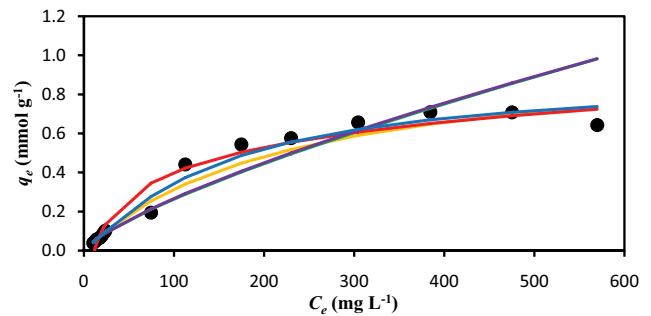


Fig. 6. Simulation plots of isotherm models: Langmuir (—), Freundlich (—), Temkin (—), R-P (—), and Sips (—) with experimental data (●) (mass of adsorbent = 0.020 g, volume of MV dye solution = 10 mL, and concentration of MV = 0–1,000 mg L⁻¹).

Depending on the type of waste being discharged, pH of wastewater varies. It has been reported that not all adsorbents are able to maintain good adsorption especially under highly acidic or basic conditions. For example, bitter melon displayed a drastic reduction of >57% toward crystal violet dye at pH 2 [54]. Investigation into the adsorption ability of KR over the range of pH from 2 to 12, as depicted in Fig. 8 (bottom), further supports KR to be a good, potential adsorbent based on the findings that it is able to consistently maintain good adsorption of >90% toward MV under various pH medium. A slight reduction in the removal of MV was observed at pH 2 which could be attributed to competing H⁺ ions for the active binding sites on KR with the cationic dye molecules. Further, MV

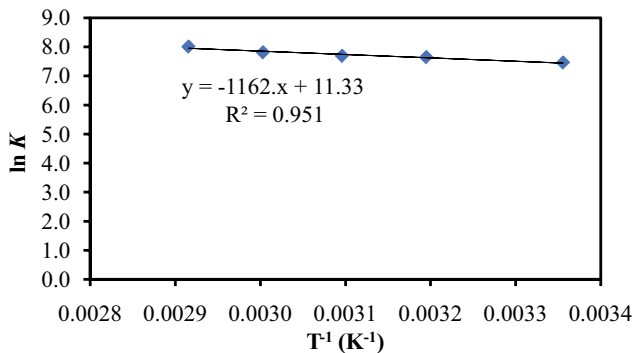


Fig. 7. van Hoff's plot of adsorption of MV by KR at temperature ranging from 298 to 343 K.

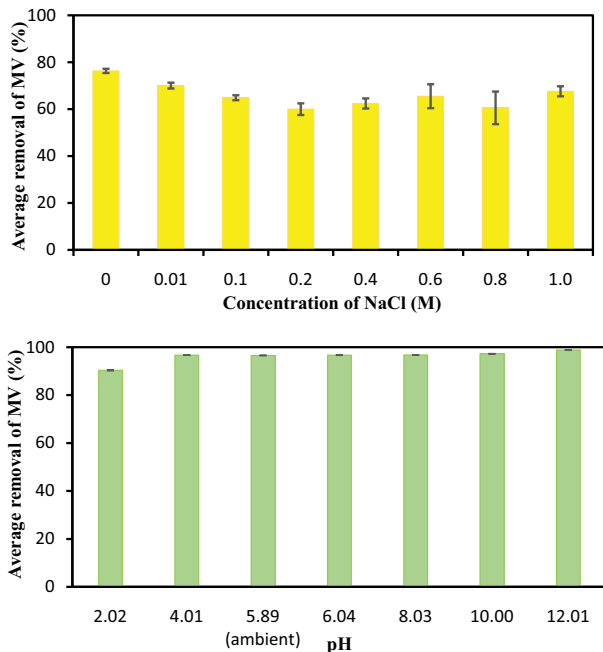


Fig. 8. Effects of ionic strength (top) and pH (bottom) on adsorption of MV onto KR (mass of adsorbent = 0.020 g, volume of MV dye solution = 10.0 mL, and concentration of MV = 100 mg L⁻¹).

being a positively charged dye could also be repelled by the H⁺ ions. At higher pH, there will be a decrease in the concentration of H⁺ ions, thereby resulting in less competition for the binding sites as well as less electrostatic repulsion with the MV dye. From this study, it must be emphasized that KR showed stability and was relatively unaffected by changes in pH, demonstrating its ability to maintain high removal of MV throughout the range studied.

3.6. Regeneration of KR

For an adsorbent to be applicable in wastewater treatment not only does it have to satisfy the criteria of having a high adsorption capacity toward pollutants but ideally it should also have the ability to be regenerated and reused in order for it to be even more cost-effective. In this study,

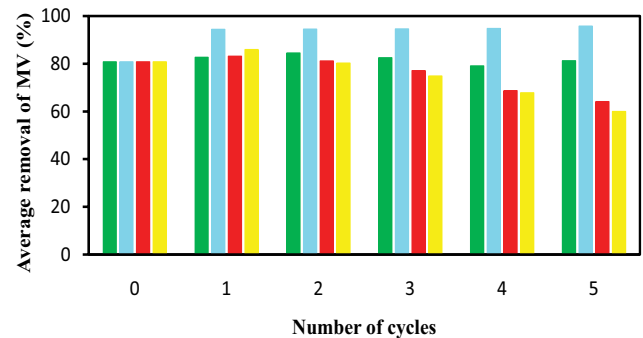


Fig. 9. Regeneration of spent KR for the adsorption of MV dye using acid (■), base (■), distilled water (■), and control experiment (■).

the investigation of the ability to regenerate and reuse the spent KR was carried out under treatment using acid, base, and distilled water. A control was also set up for comparison purposes. The results supported spent KR can be regenerated and reused, showing only 20% reduction in its adsorption toward MV in the 5th cycle (Fig. 9). Whether the spent KR was used directly or washed with distilled water prior to being used for adsorption of dye did not show much difference in the amount of dye being removed. This is significant in terms of saving both cost and time. Acid treated spent KR maintained its adsorption toward MV, whilst treatment with base enhanced its adsorption capacity even after five cycles. The above findings support the potential of KR as a potential candidate in wastewater treatment.

4. Conclusion

I. aquatica roots (KR) have proven to be an effective new low-cost adsorbent in the removal of MV dye. Amongst its attractive features is its stability when subjected to environmental changes such as pH and ionic strength, as well as its much higher adsorption capacity toward MV dye when compared to many reported adsorbents. In this respect, KR is able to maintain high removal of >90% MV dye at all the pH studied, ranging from pH 2 to 12, whilst it shows only <8% reduction when placed in 1.0 M NaCl solution. The Sips isotherm model is suitable in explaining the adsorption of MV on KR giving high q_{max} of 354.6 mg g⁻¹, which further indicates its superior adsorption ability when compared to many natural and modified adsorbents. Further, the adsorbent is able to be successfully regenerated and reused, maintaining high adsorption of >95% MV dye even after five consecutive cycles especially when using base treatment. Hence, given the above findings, *I. aquatica* roots, being inedible and readily available in abundance, could be a potential candidate as an environmental friendly and economical adsorbent in wastewater treatment.

Acknowledgment

The authors would like to thank the Government of Brunei Darussalam and Universiti Brunei Darussalam for their continuous support.

References

- [1] L. Zhu, P. Zhu, L. You, S. Li, Bamboo shoot skin: turning waste to a valuable adsorbent for the removal of cationic dye from aqueous solution, *Clean Technol. Environ. Policy*, 21 (2019) 81–92.
- [2] L.B. Carvalho, P.M.B. Chagas, L.M.A. Pinto, *Caesalpinia ferrea* fruits as a biosorbent for the removal of methylene blue dye from an aqueous medium, *Water Air Soil Pollut.*, 229 (2018) 297.
- [3] N. Priyantha, L.B.L. Lim, D.T.B. Tennakoon, M.K. Mohd Mansor, N.H. Dahri, H.I. Chieng, Breadfruit (*Artocarpus altilis*) waste for bioremediation of Cu(II) and Cd(II) ions from aqueous medium, *Ceylon J. Sci.*, 17 (2013) 19–29.
- [4] L. Zhou, H. Zhou, Y. Hu, S. Yan, J. Yang, Adsorption removal of cationic dyes from aqueous solutions using ceramic adsorbents prepared from industrial waste coal gangue, *J. Environ. Manage.*, 234 (2019) 245–252.
- [5] J. Mo, Q. Yang, N. Zhang, W. Zhang, Y. Zheng, Z. Zhang, A review on agro-industrial waste (AIW) derived adsorbents for water and wastewater treatment, *J. Environ. Manage.*, 227 (2018) 395–405.
- [6] L.B.L. Lim, N. Priyantha, K.J. Mek, N.A.H.M. Zaidi, Application of *Momordica charantia* (bitter melon) waste for the removal of malachite green dye from aqueous solution, *Desal. Water Treat.*, 154 (2019) 385–394.
- [7] A.G. Adeniyi, J.O. Ighalo, Biosorption of pollutants by plant leaves: an empirical review, *J. Environ. Chem. Eng.*, 7 (2019) 103100.
- [8] L.B.L. Lim, N. Priyantha, D.T.B. Tennakoon, C. Hei Ing, C. Bandara, Sorption characteristics of peat of Brunei Darussalam I: characterization of peat and adsorption equilibrium studies of methylene blue-peat interactions sodium hydroxide modified rice husk for enhanced removal of copper ions view project development of I, *Ceylon J. Sci.*, 17 (2013) 41–51.
- [9] G. Bayazit, Ü.D. Gül, D. Ünal, Biosorption of acid red P-2BX by lichens as low-cost biosorbents, *Int. J. Environ. Stud.*, 76 (2019) 603–615.
- [10] L. Bulgariu, B. Cojocariu, A.M. Mocanu, G. Nacu, Possible utilization of PET waste as adsorbent for Orange G dye removal from aqueous media, *Desal. Water Treat.*, 104 (2018) 338–345.
- [11] L. Yang, Y. Wang, A. Liu, Y. Zhang, CoO₂/MoO₄-anchored multi-wrinkled biomass carbon as a promising material for rapidly selective methyl blue removal, *J. Mater. Sci.*, 54 (2019) 11024–11036.
- [12] H. Li, Y. Li, Y. Chen, M. Yin, T. Jia, S. He, Q. Deng, S. Wang, Carbon tube clusters with nanometer walls thickness, micrometer diameter from biomass, and its adsorption property as bioadsorbent, *ACS Sustainable Chem. Eng.*, 7 (2019) 858–866.
- [13] M.S. Alhumaimess, Sulfhydryl functionalized activated carbon for Pb(II) ions removal: kinetics, isotherms, and mechanism, *Sep. Sci. Technol.*, 55 (2019) 1303–1316.
- [14] V. Kumar, V. Rehani, B.S. Kaith, S. Saruchi, Synthesis of a biodegradable interpenetrating polymer network of Av-cl-poly(AA-*ipn*-AAm) for malachite green dye removal: kinetics and thermodynamic studies, *RSC Adv.*, 8 (2018) 41920–41937.
- [15] T. Zehra, N. Priyantha, L.B.L. Lim, Removal of crystal violet dye from aqueous solution using yeast-treated peat as adsorbent: thermodynamics, kinetics, and equilibrium studies, *Environ. Earth Sci.*, 75 (2016) 1–15.
- [16] L. Bedabati Chanu, A. Gupta, Phytoremediation of lead using *Ipomoea aquatica* Forsk. in hydroponic solution, *Chemosphere*, 156 (2016) 407–411.
- [17] A. Weerasinghe, S. Ariyawansa, R. Weerasooriya, Phytoremediation potential of *Ipomoea aquatica* for Cr(VI) mitigation, *Chemosphere*, 70 (2008) 521–524.
- [18] K.S. Wang, L.C. Huang, H.S. Lee, P.Y. Chen, S.H. Chang, Phytoextraction of cadmium by *Ipomoea aquatica* (water spinach) in hydroponic solution: effects of cadmium speciation, *Chemosphere*, 72 (2008) 666–672.
- [19] J.C. Chen, K.S. Wang, H. Chen, C.Y. Lu, L.C. Huang, H.C. Li, T.H. Peng, S.H. Chang, Phytoremediation of Cr(III) by *Ipomoea aquatica* (water spinach) from water in the presence of EDTA and chloride: effects of Cr speciation, *Bioresour. Technol.*, 101 (2010) 3033–3039.
- [20] M.A. Rahman, H. Hasegawa, Aquatic arsenic: phytoremediation using floating macrophytes, *Chemosphere*, 83 (2011) 633–646.
- [21] M.B. Kurade, J.Q. Xiong, S.P. Govindwar, H.S. Roh, G.D. Saratale, B.H. Jeon, H. Lim, Uptake and biodegradation of emerging contaminant sulfamethoxazole from aqueous phase using *Ipomoea aquatica*, *Chemosphere*, 225 (2019) 696–704.
- [22] N.R. Rane, S.M. Patil, V.V. Chandanshive, S.K. Kadam, R.V. Khandare, J.P. Jadhav, S.P. Govindwar, *Ipomoea hederifolia* rooted soil bed and *Ipomoea aquatica* rhizofiltration coupled phytoreactors for efficient treatment of textile wastewater, *Water Res.*, 96 (2016) 1–11.
- [23] Q. Zhang, V. Achal, Y. Xu, W.N. Xiang, Aquaculture wastewater quality improvement by water spinach (*Ipomoea aquatica* Forsskal) floating bed and ecological benefit assessment in ecological agriculture district, *Aquacult. Eng.*, 60 (2014) 48–55.
- [24] M. Li, Y.J. Wu, Z.L. Yu, G.P. Sheng, H.Q. Yu, Enhanced nitrogen and phosphorus removal from eutrophic lake water by *Ipomoea aquatica* with low-energy ion implantation, *Water Res.*, 43 (2009) 1247–1256.
- [25] B.H. Hameed, Equilibrium and kinetic studies of methyl violet sorption by agricultural waste, *J. Hazard. Mater.*, 154 (2008) 204–212.
- [26] J. Li, D.H.L. Ng, P. Song, C. Kong, Y. Song, Synthesis of SnO₂-activated carbon fiber hybrid catalyst for the removal of methyl violet from water, *Mater. Sci. Eng.*, B, 194 (2015) 1–8.
- [27] S. Lagergren, About the theory of so-called adsorption of soluble substances, *K. Sven. Vetensk. Akad. Handl.*, 24 (1898) 1–39.
- [28] Y.S. Ho, G. McKay, Sorption of dye from aqueous solution by peat, *Chem. Eng. J.*, 70 (1998) 115–124.
- [29] S.Z. Roginsky, J. Zeldovich, Über den mechanismus der katalytischen von CO an MnO₂, *Acta Physicochim.*, 1 (1934) 554–594.
- [30] M.A. Hubbe, S. Azizian, S. Douven, Implications of apparent pseudo-second-order adsorption kinetics onto cellulosic materials: a review, *Bioresources*, 14 (2019) 7582–7626.
- [31] K.L. Tan, B.H. Hameed, Insight into the adsorption kinetics models for the removal of contaminants from aqueous solutions, *J. Taiwan Inst. Chem. Eng.*, 74 (2017) 25–48.
- [32] F.C. Wu, R.L. Tseng, R.S. Juang, Initial behavior of intraparticle diffusion model used in the description of adsorption kinetics, *Chem. Eng. J.*, 153 (2009) 1–8.
- [33] L.B.L. Lim, N. Priyantha, N.A.H. Mohamad Zaidi, A superb modified new adsorbent, *Artocarpus odoratissimus* leaves, for removal of cationic methyl violet 2B dye, *Environ. Earth Sci.*, 75 (2016) 1–13.
- [34] L.B.L. Lim, N. Priyantha, C.M. Chan, D. Matassan, H.I. Chieng, M.R.R. Kooh, Adsorption behavior of methyl violet 2B using duckweed: equilibrium and kinetics studies, *Arabian J. Sci. Eng.*, 39 (2014) 6757–6765.
- [35] L.B.L. Lim, N. Priyantha, C.M. Chan, D. Matassan, H.I. Chieng, M.R.R. Kooh, Investigation of the sorption characteristics of water lettuce (WL) as a potential low-cost biosorbent for the removal of methyl violet 2B, *Desal. Water Treat.*, 57 (2016) 8319–8329.
- [36] C. Duran, D. Ozdes, A. Gundogdu, H.B. Senturk, Kinetics and isotherm analysis of basic dyes adsorption onto almond shell (*Prunus dulcis*) as a low cost adsorbent, *J. Chem. Eng. Data*, 56 (2011) 2136–2147.
- [37] Y. Wang, Y. Xie, Y. Zhang, S. Tang, C. Guo, J. Wu, R. Lau, Anionic and cationic dyes adsorption on porous poly-melamine-formaldehyde polymer, *Chem. Eng. Res. Des.*, 114 (2016) 258–267.
- [38] M.K. Dahri, M.R.R. Kooh, L.B.L. Lim, Removal of methyl violet 2B from aqueous solution using *Casuarina equisetifolia* needle, *ISRN Environ. Chem.*, 2013 (2013) 1–8.
- [39] M.K. Dahri, H.I. Chieng, L.B.L. Lim, N. Priyantha, C.C. Mei, Cempedak durian (*Artocarpus* sp.) peel as a biosorbent for the removal of toxic methyl violet 2B from aqueous solution, *Korean Chem. Eng. Res.*, 53 (2015) 576–583.

- [40] L.B.L. Lim, N. Priyantha, C.H. Ing, M.K. Dahri, D.T.B. Tennakoon, T. Zehra, M. Suklueng, *Artocarpus odoratissimus* skin as a potential low-cost biosorbent for the removal of methylene blue and methyl violet 2B, *Desal. Water Treat.*, 53 (2013) 964–975.
- [41] P. Li, Y.J. Su, Y. Wang, B. Liu, L.M. Sun, Bioadsorption of methyl violet from aqueous solution onto Pu-erh tea powder, *J. Hazard. Mater.*, 179 (2010) 43–48.
- [42] M.R.R. Kooh, M.K. Dahri, L.B.L. Lim, Removal of methyl violet 2B dye from aqueous solution using *Nepenthes rafflesiana* pitcher and leaves, *Appl. Water Sci.*, 7 (2017) 3859–3868.
- [43] M.K. Dahri, M.R.R. Kooh, L.B.L. Lim, Artificial neural network approach for modelling of methyl violet 2B dye adsorption using pomelo skin, *J. Environ. Biotechnol. Res.*, 6 (2017) 238–247.
- [44] L.B.L. Lim, N. Priyantha, Y.C. Lu, N.A.H.M. Zaidi, Effective removal of methyl violet dye using pomelo leaves as a new low-cost adsorbent, *Desal. Water Treat.*, 110 (2018) 264–274.
- [45] M.I. Din, K. Ijaz, K. Naseem, Biosorption potentials of acid modified *Saccharum bengalense* for removal of methyl violet from aqueous solutions, *Chem. Ind. Chem. Eng. Q.*, 23 (2017) 399–409.
- [46] N.A.H.M. Zaidi, L.B.L. Lim, A. Usman, *Artocarpus odoratissimus* leaf-based cellulose as adsorbent for removal of methyl violet and crystal violet dyes from aqueous solution, *Cellulose*, 25 (2018) 3037–3049.
- [47] L.R. Bonetto, F. Ferrarini, C. de Marco, J.S. Crespo, R. Guégan, M. Giovanela, Removal of methyl violet 2B dye from aqueous solution using a magnetic composite as an adsorbent, *J. Water Process Eng.*, 6 (2015) 11–20.
- [48] S. Azizian, M. Haerifar, H. Bashiri, Adsorption of methyl violet onto granular activated carbon: equilibrium, kinetics and modeling, *Chem. Eng. J.*, 146 (2009) 36–41.
- [49] Y. Kim, J. Bae, H. Park, J.K. Suh, Y.W. You, H. Choi, Adsorption dynamics of methyl violet onto granulated mesoporous carbon: facile synthesis and adsorption kinetics, *Water Res.*, 101 (2016) 187–194.
- [50] A. Guzmán-Vargas, E. Lima, G.A. Uriostegui-Ortega, M.A. Oliver-Tolentino, E.E. Rodríguez, Adsorption and subsequent partial photodegradation of methyl violet 2B on Cu/Al layered double hydroxides, *Appl. Surf. Sci.*, 363 (2016) 372–380.
- [51] M.R.R. Kooh, M.K. Dahri, L.B.L. Lim, L.H. Lim, O.A. Malik, Batch adsorption studies of the removal of methyl violet 2B by soya bean waste: isotherm, kinetics and artificial neural network modelling, *Environ. Earth Sci.*, 75 (2016) 1–14.
- [52] M.R.R. Kooh, M.K. Dahri, L.B.L. Lim, Removal of the methyl violet 2B dye from aqueous solution using sustainable adsorbent *Artocarpus odoratissimus* stem axis, *Appl. Water Sci.*, 7 (2016) 3573–3581.
- [53] M.K. Dahri, M.R.R. Kooh, L.B.L. Lim, Adsorption of toxic methyl violet 2B dye from aqueous solution using *Artocarpus heterophyllus* (jackfruit) seed as an adsorbent, *Am. Chem. Sci. J.*, 15 (2016) 1–12.
- [54] L.B.L. Lim, N. Priyantha, K.J. Mek, N.A.H.M. Zaidi, Potential use of momordica charantia (bitter gourd) waste as a low-cost adsorbent to remove toxic crystal violet dye, *Desal. Water Treat.*, 82 (2017) 121–130.